Mehran University Research Journal of Engineering and Technology

https://doi.org/10.22581/muet1982.2202.03

2022, 41(2) 21-34

Sensitivity analysis and optimization of land use/cover and aquifer parameters for improved calibration of hydrological model

Ammara Nusrat [a,*], Hamza Farooq Gabriel [a], Sajjad Haider [a], Mohsin Siddique [b]

[a] *Institute of Civil Engineering, National University of Sciences and Technology, Islamabad Pakistan*

[b] *Ministry of the Environment, Conservation and Parks, Ontario Canada*

[*] Corresponding author: Ammara Nusrata, Email: ammara@nice.nust.edu.pk

Received: 25 July 2019, Accepted: 30 November 2021, Published: 01 April 2022

K E Y W O R D S

Hydrological Modeling

Sensitivity Analysis

Optimization

Parameter Ranking

Calibration

A B S T R A C T

Integrated Flood Analysis System (IFAS) model, based on Tank model philosophy, is a widely used flood forecasting model that has the capability to simulate the catchment processes of any river system provided the surface and aquifer parameters of each sub-model are accurately calibrated. In this study, sensitivity analysis and optimization of hydrogeological parameters of Tank model have been performed to identify the key hydrogeological parameters and their significance in simulating the stream flows in the basins of two important rivers of Pakistan – Jhelum River and Chenab Rivers – respectively. IFAS includes a set of four sub-models namely: surface tank model, sub-surface tank model, aquifer tank model and river course model. Each of the sub-models simulates its own flow processes using surface/aquifer parameters. In this study, sensitivity analysis is performed to identify the parameters that significantly affect the model performance to simulate the flows in the river. Linear stochastic metamodels of Jhelum River and Chenab River Basins developed in this study played the role of metamodels or surrogate functions to determine the ranges of parameter values in different flow periods. The outcome demonstrates when the aquifer tank parameters values obtained from metamodels are applied, the simulation results in a nearly accurate calibration, which clearly indicates the efficiency of present methodology and the important role of hydrogeological parameters. Further, the analysis of the variability in the effectiveness of these parameters in different flow periods as well as for different catchments areas depicts spatial-temporal heterogeneous characteristics. This confirms that the analysis should be directed independently for each study basin because the results of sensitivity analysis are not transferable among catchments.

1. Introduction

The evaluation of computational efficiency of complex hydrological models and sensitivity analysis are the obligatory problems even with high performance computational infrastructure [1]. Physically-based predictions are required for practical hydrological problems. Realistic estimates of the physically based model uncertainty to assess future scenarios that affect the management strategies are really the utmost necessity to improve the quality of models.

Parameter sensitivity analysis, and optimization are the approaches which are very important for robust and reliable hydrologic models' predictions [2-3]. It is also important to analyse parameters' interconnections that influence the prognostic execution of the hydrological models [4]. The uncertainties are related to the input parameters of computational models, which are further associated with the decision-making, prediction and planning. The parameters sensitivity and uncertainty analyses of these computational models are important before and during its application for forecasting, design and planning. The present physically based models and their enhanced capabilities of integrating highly spatially and temporally resolved data and numerous input parameters, are computationally demanding and costly. Consequently, the conventional hit and trial methods have proved to be time consuming and arduous. Different optimization methods are integrated with conceptual and distributed hydrological models but they face constraints of computational time. There is a need of a robust strategy which not only optimizes the input parameters for accurate calibration but also reduces the extensive computational requirements of the model by using some surrogate models also called as metamodels.

Metamodeling is an undeniably popular methodology for easing the computational demand. The metamodeling approach is also referred to as surrogate modelling, function approximation, model emulation or response surface method. The objective function of optimization, termed as metamodel, is an output driven function, which omits the need to always calculate the output by means of a computationally costly simulation runs [2]. Many metamodeling techniques have been applied in many environmental and water resources related problems like model calibration, design and optimization of water distribution network system, water system analysis and management. Saman et al [2] presented the detailed review of the literature which applied metamodeling strategies for the enhanced efficiency of the solution through computationally intensive problems. Metamodels are used for optimization by furnishing a deterministic target function with run times that are commonly a lot shorter than the first discrete-occasion simulation. Gauchi et al. [5] presented the multi-objective method in which metamodeling and sensitivity analysis have been performed simultaneously. They optimized the model input parameters, using the objective function of sensitivity indices.

In hydrological models, numerous input parameters need to be estimated for accurate calibration of the model. Many researchers have devised number of methods to estimate and optimize the input parameters for computational cost reduction which are induced due to running the hydrological model numerous times. Boyel et al. [6] and Hogue et al. [7] divided the hydrograph and integrated the optimization method with the expert knowledge for better calibration of the hydrological model. Step-wise calibration techniques were used by many investigators [8-10] in which objective functions for the optimization of the parameters were linked with different hydrological process. In many of the past studies, a number of global and local optimization techniques have been applied, with the aim to find the parameters' importance and sensitivities in the hydrological model in order to reduce the computational cost [8-9]. However, in the physical based distributed model, which is highly resolved, the parameterization and optimization are difficult and challenging tasks.

A regression metamodel can be used in the assessment of simulation results as linear regression analysis is significant in numerous fields [11-13]. Modelers utilized direct regression metamodeling as an instrument to build understanding of computationally intensive models and better impart their outcomes [14]. The ranges of highly ranked parameters were used for robust and improved hydrological model calibration. The identification of highly sensitive parameters is the first objective of the study.

The research questions which have been addressed in the present study are: (1) what are the most sensitive hydrogeological parameters in the Integrated Flood Analysis System (IFAS) model, whose variability can affect the model output, i.e. the streamflow, considerably in different flow periods? (2) Are the sensitivity indices corresponding to different parameters the same for all flow periods? (3) Are the sensitivities of these parameters different for different catchments? (4) What is the role of hydrogeological parameters in simulating the streamflow in high and low flow periods? (5) Would a surrogate model for optimization of the parameters, be effective in reducing the simulation runs and time? (6) How these surrogate models or metamodels for highly ranked parameters are improving the optimization and calibration processes?

In order to identify the variability in the effectiveness of the parameters in different flow periods, the Monsoon season has been divided in low flow period, high flow period and post flood or recession period, which presents temporal changes in the importance of the parameters. Two basins – Jhelum River Basin and Chenab Rivers Basin – are considered to analyse the spatial change in the sensitivities of the parameters.

2. Materials and Methods

2.1 Description of Integrated Flood Analysis Model

An efficient measure, to reduce the damages during flood hazards, particularly in scarcely gauged river basin, depends upon the capability of systems used for flood warning and forecasting. The IFAS model [15], used in the present study, is an efficient flood forecasting model. It works on the principles of tank model for prediction of runoff while for flood routing it uses kinematic wave model. Tank model non-linear relationships, based on Manning and hyperbolic approximations, are used to calculate the outflow from each tank [16-18]. IFAS uses a four-layer non-linear tank structure to minimize the simulations time [15].

The tank model introduced by Sugawara [16] includes four tanks to analyse daily discharges. According to him, different hydrological processes occur in different tanks namely, surface tank, sub-surface tank, aquifer tank and river tank. Each tank contributes towards the flow in the river. This model can include infiltration, water storages, and percolation processes. It has been used by many investigators and researchers to simulate and analyse the rainfall – runoff processes in various basins for different periods [16-22]. Fig. 1 shows the illustration of Tank Model showing parameters and classification. The values of tank model parameters such as initial storage, height of tank, and coefficients, number and layers of tank model, have been reported by many researchers, and can be used as reference values [17-22].

IFAS is a Distributed Hydrological Model. To uniquely represent physical characteristics of the river system and the movement processes by different functions [15] it requires huge spatial data such as river shape, geology, slopes, soil, snow cover [15-20]. IFAS is capable to simulate stream flows, subsurface and aquifer flow, through nonlinear 2 or 3 layer tanks structure. It uses approximation functions to solve the time integral equation using numerical solutions. To calculate discharge in the river course tank, IFAS solves kinematic wave equation to calculate discharge in the river. IFAS uses total rainfall as input and gives total runoff as output along with values of different components viz. surface flow, subsurface flow, and base flow separately. IFAS allows the users to vary the parameters according to land use/cover, geology and soil of the watershed area. In IFAS, parameters can roughly be estimated using grid-based global data sets on topography, soil, geology, land use. The equations to calculate the discharges in a particular tank in IFAS model are discussed in the following sub-section:

2.1.1 Surface tank model

Three flows are involved in Surface tank model: Saturation Excess Overland/ surface Flow, Rapid Subsurface Flow and Infiltration. The detail description of each model is given below.

2.1.1.1 Saturation excess overland flow: In surface tank model, rainfall is divided in three flows i.e. surface flow or overland flow, intermediate flow and infiltration. Eq. 1 gives the formula for overland flow Q_{sf} (m^3/s).

$$Q_{sf} = L\frac{1}{SNF}\,(h - HFMXD)^{\frac{5}{3}}(\sqrt{i}) \tag{1}$$

where, L is cell length (m) of the simulation model, h is depth of water (m), SNF is coefficient of surface roughness in $m^{-1/3}s$, HFMXD is maximum height of water of surface tank (m), i is surface slope. When the value of maximum storage height of water (HFMXD) is increased, the overland flow generation is delayed, and when it is decreased, overland flow is accelerated. Discharges from tank, topography and land use are responsible for the increase or decrease of peak discharge.

2.1.1.2 Rapid subsurface flow: Eq. 2 provides the formula for the calculation of rapid subsurface flow Q_{rf} (m^3/s).

$$Q_{rf} = FALFX\,[A]\,[SKF]\,\frac{(h-HFMND)}{(HFMXD-HFMND)} \tag{2}$$

where, *FALFX* is rapid intermediate flow regulation coefficient, *HFMND* is height where rapid intermediate flow occurs (m), A is the wetted area of the tank (m^2), *SKF* is final infiltration capacity (cm/s).

When the value of *SKF* is increased, the storage height of the aquifer tank is increased. This is effective when the flood hydrograph is to be increased in recession period or delaying peak since this increases discharge from aquifer layer tank. When the value is decreased, storage height of the surface layer tank is increased.

2.1.1.3 Infiltration: Darcy Law has been used to calculate infiltration as a part of storage capacity. Eq. 3 calculates the infiltration Q_O (m^3/s).

$$Qo = [A]\,[SKF]\,\frac{(h-HFOD)}{(HFMXD-HFMND)} \tag{3}$$

where, *HFOD* is the height where ground infiltration occurs.

The low flow conditions and long-term periods are simulated by unsaturated tank model.

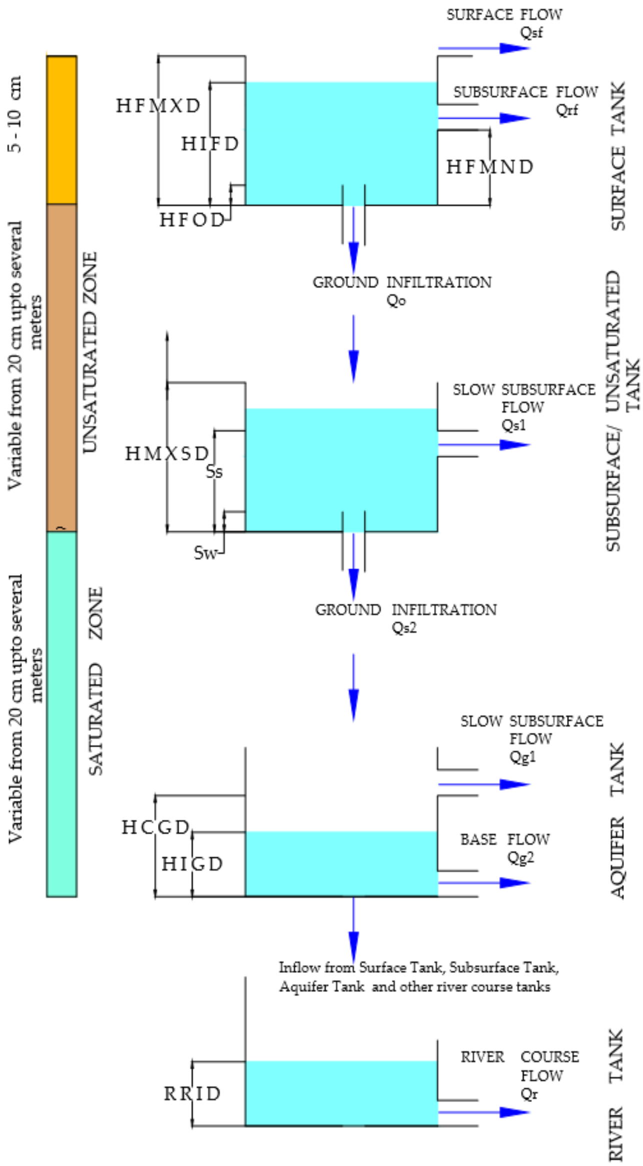

Fig. 1. Schematic configuration of IFAS model showing the classification of surface/subsurface zones

2.1.2 Sub-surface tank model

Two flows are involved in sub-surface tank model: Slow sub-surface flow and Infiltration to aquifer. Slow subsurface storm flow, Q_{s1} is based on Darcy's law and lateral flow. It is one of the component of processes in sub-surface tank model. Eqs. 4-5 are used to calculate this slow subsurface storm flow.

$$Q_{s1} = [K_x]\, D\, i \tag{4}$$

$$K_x = \frac{SKX}{100} \cdot \frac{\exp(b.\theta) - \exp(b.\theta_W)}{\exp(b.\theta_s) - \exp(b.\theta_W)} \tag{5}$$

Infiltration to aquifer, Q_{s2} (in m^3/s) is vertical flow to the underlying aquifer tank from the sub-surface tank and is calculated using Eqs. 6-7.

$$Q_{s2} = A\,[K_z]\, i \tag{6}$$

$$K_z = SKD.\frac{\exp(b.\theta) - \exp(b.\theta_W)}{\exp(b.\theta_s) - \exp(b.\theta_W)} \tag{7}$$

where, D is total water height (m) for unsaturated tank, θ is soil moisture content (= h/D), S_S is height (m) when $\theta = \theta_S$, θ_S is saturated soil moisture (= S_S/D), S_W is height (m) when $\theta = \theta_W$, θ_W is wilting point soil moisture (= S_W/D), K_X (cm/s) is horizontal hydraulic conductivity at θ, SKX is the horizontal hydraulic conductivity (cm/s) at θ_S, K_z is vertical hydraulic conductivity (cm/s) at θ, SKD is vertical permeability (cm/s) and b is a constant based on soil total porosity and ranges from 0-100 [15].

2.1.3 Aquifer tank model

Aquifer layer tank has two orifices for unconfined aquifer outflow and confined aquifer outflow. The outflow from the unconfined aquifer, Q_{g1} (m^3/s), and confined aquifer outflow, Q_{g2}(m^3/s), are calculated using Eqs. 10-11 respectively. The height of water in the tank, h, varies with time and is determined by Eqs. 8-9.

$If\ h \geq HCGD,\ then$

$$\frac{\partial h}{\partial t} A = Q_{s2} - Q_{g1} - Q_{g2} - Q_{g-loss} \tag{8}$$

$If\ h < HCGD,\ then$

$$\frac{\partial h}{\partial t} A = Q_{s2} - Q_{g2} - Q_{g-loss} \tag{9}$$

$$Q_{g1} = [AUD]^2(\mathrm{HIGD} - \mathrm{HCGD})^2 A \tag{10}$$

$$Q_{g2} = [AGD]\, hA \tag{11}$$

where, AUD is the unconfined streamflow coefficient (1/mm/day)$^{1/2}$, AGD is the confined aquifer streamflow coefficient (1/day), $HCGD$ is the height where the unconfined aquifer runs off (m) and $HIGD$ is initial water height (m), A is the wetted area (m^2) and Q_{g-loss} is unaccountable aquifer loss.

2.1.4 River course tank model

Outflow from the river tank is based on Manning equation represented by Eq. 12. River course with compound sections are also calculated within this model.

$$Q_r = B\frac{1}{n}h^{5/3}\sqrt{i} \tag{12}$$

where, Q_r is the outflow from the river course (m^3/s), L is the length, i is the gradient of riverbed, B is the breath of river course. The river course breath is calculated with the help of resume law [15].

2.2 Methods

The methodology includes the estimation of sensitivities of parameter for different basins, and the optimization of the parameters using linear regression metamodels obtained from the sensitivity experiments, which served as the tool for better calibration of the model. Daily rainfall observed data of the monsoon season of the year 2014, soil, geology, land use, elevations, and snow cover were imported in the IFAS model. Out of all parameters, ten uncertain parameters related to surface, aquifer and river layer tank, are selected for sensitivity analysis. The detail of the surface and the aquifer tank parameters of IFAS, considered in sensitivity analysis is given in Tables 1 and 2. Parameters sets are developed for local sensitivity analysis using one-at-a-time (OAT) sampling method, assuming that the selected input parameters for this analysis are not inter-dependent [23].

Each model parameter is sampled for 22 values in its specified space, the criteria of number of evaluations for local sensitivity analysis was explained by Pianosi et al. [23]. Sensitivities of 10 parameters are investigated using 220 model simulations. The daily runoffs were reported for the two watersheds, for each of these 220 simulations. The unique feature of the present study is the ranking of the parameters through different sensitivity analysis experiments namely Kolmogorov-Smirnoff test, amplification factor experiment, spider plots and performance plots for different flow regimes, in order to find the most sensitive parameters in the model. Finally, using the sensitivity and regression analysis results, the metamodels are developed for the highly sensitive parameters and the optimal ranges of the influential parameters are proposed for the two study basins.

2.2.1 Parameter sensitivity estimation

Sensitivity analysis is performed for the identification of the parameters that influence the model outcome. It is generally acknowledged that recognizing the most significant parameters is important for hydrological modelling, challenging parameterization and improvement of model itself. Song et al. [1] presented comprehensive study and review of different methods of sensitivity analysis used for hydrological modelling. They outlined the framework of global sensitivity analysis. Wang [4] presented the application of probabilistic framework by merging two methods to quantify the uncertainties in the hydrological model. Benke et al. [24] determined parameters uncertainty using different simulation experiments and Monte Carlo distribution of the parameters, and found out that the shape of the parameter distribution has great influence on the model uncertainty calculations.

Table 1

Surface Layer Tank Parameters Included In Sensitivity Analysis

Parameter	Symbol
Final Infiltration Capacity	SKF (cm/s)
Height responsible for ground infiltration	HFOD (m)
Maximum Height of Water	HFMXD (m)
Height responsible for Intermediate rapid flow	HFMND (m)
Subsurface Runoff Coefficient	FALFX (n)
Manning's coefficient of roughness	n ($m^{-1/3}$/s)

According to OAT investigation at the point when the affectability for one parameter is being resolved, values for that parameter were changed and constant appropriate values are assigned to every other parameter for the specific basin under investigation. Different sensitivity indices are used in the present study (1) to rank the parameters in different flow regimes of the monsoon season of year 2014 and (2) to rank the parameters in the whole monsoon season using performance and probability plots.

Table 2

Aquifer Layer Tank Parameters Included In Sensitivity Analysis

Parameter	Symbol
un-confined aquifer -Streamflow coefficient	AUD (1/mm/day$^{1/2}$)
confined aquifer streamflow coefficient	AGD (1/day)
Height responsible for unconfined aquifer runs off	HCGD (m)
Initial water height	HIGD (m)

2.2.1.1 Sensitivity indices in different flow regimes: Amplication factor and deterministic index are used to evaluate the parameters' sensitivities at different flow regimes in both watershed. Amplification factor also sensitivity index is based on coefficient of variation of parameters and output and is calculated using Eq. 13.

$$[S_A]_i = \frac{\partial[\mathrm{CV}_{output}]_i}{\partial[\mathrm{CV}_{parameter}]} \qquad (13)$$

where, S_A is the amplification factor, CV_{output} is the coefficient of variation [25] in percentage for the output, and $CV_{parameter}$ is the coefficient of variation of input parameter in percentage. Subscript i is for specific percentile of the output.

The following Eq. 14 is used to calculate the deterministic index.

$$[S_s]_i = \frac{\partial[O_c]_i}{\partial[P_c]} \qquad (14)$$

where, S_s is the deterministic index, O_c is the % change in model output, and P_c is the % change in parameter input.

2.2.1.2 Ranking of parameters using probability plots: IFAS Model simulations were performed using one at a time (OAT) sampling method. It means that for every change in the parameter value, we will have one set of daily stream flows for the whole monsoon season. Eq. 16 gives the test statistics of *KS* test. According to the *KS* test, larger the vertical maximum distance between the two cumulative frequencies, x_i, the more sensitive the factor is. KS index is defined as follows [26].

$$KS(x_i) = max\left|F_y(y) - F_{y/xi}(y)\right| \tag{15}$$

where, $F_y(y)$ is the output streamflow cumulative probability distribution function, and the $F_{y/xi}(y)$ is the conditional output cumulative distribution function when xi is fixed.

$$\hat{T}_i = \underbrace{stat}_{x_i=\bar{x}_i{}^1,\bar{x}_i{}^2,\ldots,\bar{x}_i{}^n} \left[\left(KS(x_i)\right)\right] \tag{16}$$

where, $\hat{T}$ is PAWN index [26], as test statistics, which has been used for ranking of the parameters, $\bar{x}_i{}^1, \bar{x}_i{}^2, \ldots, \bar{x}_i{}^n$ are n values for input parameter.

The $\hat{T}$ value varies from 0 to 1. The greater value represents greater sensitivity of the parameter. **Error! Reference source not found.** shows the summary of the steps used to perform this test.

2.2.1.3 Ranking of parameters through performance plots' slopes: Ranking of the parameters is based on the change in model performance indicators with a unit change in parameters value. Observed and simulated flow data have been used to calculate the model performance indices. The selection of suitable model error measure and the performance indicators is very important for effective model parameter calibration [27]. The ranking of the parameters in IFAS model was performed by evaluating the slopes of performance plots. Performance indices were calculated for each model run and observed data. The Table 3 shows the list of model performance indicators and their formulation.

The rate of change of performance metrics per unit change in parameter value is computed using Equation (17).

$$P_s = \frac{\partial[M]_c}{\partial[P_c]} \tag{17}$$

where, P_s is the Performance slope index, $[M]_c$ is the performance metrics, and P_c is the percentage change in the parameter value. Subscript "c" is for specific parameter. The weights assigned to each experiment depends upon the co-linearity between the two variables used in the particular experiment.

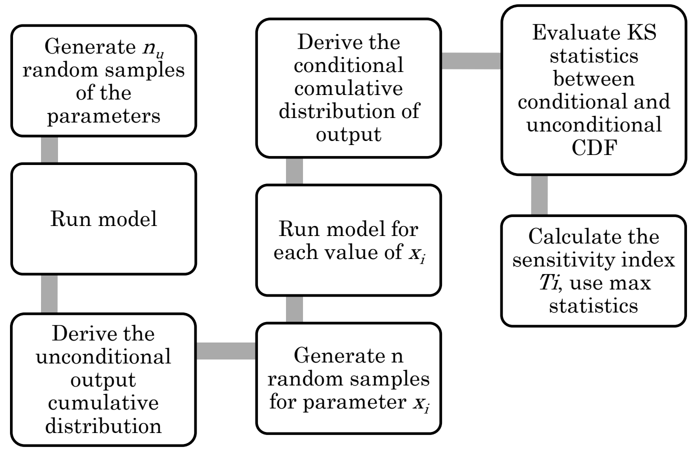

Fig. 2. Steps used to perform Kolmogorov Smirnov test

(Oi = Observed flow for ith day, Pi=Predicted flow by the model for ith day, $\overline{O}$ = Mean of observed flow, and N = total number of time steps for one simulation run)

2.2.4 Weighted average ranking

The overall raking has been calculated using weighted average ranking (WAR) method [28] for all the sensitivity experiments. Table 4 provides the detail of the weights given to ranking of parameter for individual experiment.

2.2.5 Optimal parameterization and interpolation through metamodels on analysis

The metamodels with high linear correlation, so obtained, from deterministic index function and amplification index function, were analysed and interpolated to determine ranges of parameter values in different flow periods. Different Replacement algorithms are used in optimization techniques [12]. The advantage of meta-modelling is to decrease the overall running time, by simplifying the complex model [29].

2.3 Data and Materials

Model simulations output quality is greatly affected by the quality, nature and availability of geospatial and hydro-meteorological data [20]. This part looks at the accessibility and nature of different data.

2.3.1 Study area

The Jhelum River is a major eastern tributary of the large Indus Basin Irrigation System (IBIS). It rises from the high-elevation snow-fed Himalayan and Pir Panjal ranges and receives inflow from four major tributaries: the Neelum/ Kishanganga, Naran, Poonch, and Kanshi Rivers. The Mangla Dam is the only rim station on Jhelum

River and the confluence point of all the aforementioned tributaries. The present study is conducted in the Jhelum River Basin up to the Mangla Dam (Basin area: 33,867 km^2). Mean annual precipitation fluctuates between 880mm to 1330mm in various parts of the catchment [30]. The Chenab watershed is approximately 67,515 Km^2. The total basin area upstream of Maralla Barrage is almost 28,000 km^2. Fig. 3-4 shows the location and digital elevation model (DEM) of Jhelum River Basin and Chenab River Basin respectively, the flow measuring stations in both basins have also been pointed out. Fig. 5 (A-B) shows the land use/cover classification of the area used in IFAS model for flow simulations.

Table 3

Model performance indices used in the present study

Description	Equations
Relative Index of Agreement	$d_{rel} = 1 - \frac{\sum_{i=1}^{N}\left[\frac{O_i - P_i}{O_i}\right]^2}{\sum_{i=1}^{N}\left[\frac{\lvert P_i - \bar{O}\rvert + \lvert O_i - \bar{O}\rvert}{\bar{O}}\right]^2}$
Modeling Efficiency	$EF = \frac{\sum_{i=1}^{N}(O_i - \bar{O})^2 - \sum_{i=1}^{N}(P_i - O_i)^2}{\sum_{i=1}^{N}(O_i - \bar{O})^2}$
Wave shape error	$E_w = \frac{1}{N}\sum_{i=1}^{N}\left[\frac{O_i - P_i}{O_i}\right]^2$
Volume error	$E_v = \frac{\sum_{i=1}^{N} O_i - \sum_{i=1}^{N} P_i}{\sum_{i=1}^{N} O_i}$
Peak discharge error	$E_P = \frac{O_{peak} - P_{peak}}{O_{peak}}$
Root Mean Square Error (m^3/s)	$RMSE = \sqrt{\frac{\sum_{i=1}^{N}(O_i - P_i)^2}{N}}$
RMSE/STDEV$_{obs}$	$RSR = \frac{\sqrt{\sum_{i=1}^{N}(O_i - P_i)^2}}{\sqrt{\sum_{i=1}^{N}(O_i - \bar{O})^2}}$
Fourth Root Mean Quadrupled Error (m^3/s)	$R4MS4E = \sqrt[4]{\frac{\sum_{i=1}^{N}[O_i - P_i]^4}{n}}$
Percent Bias	$PBIAS = \frac{\sum_{i=1}^{N}(O_i - P_i)}{\sum_{i=1}^{N} O_i} \times 100$

Table 4

Weights given to ranking of parameter for individual experiment

Sensitivity Experiments	Weights	Sensitivity Experiments	Weights
$[S_s]_i$	0.85	RSR	0.33
$[S_A]_i$	0.86	R4MS4E	0.97
$\hat{T}_i$	0.85	PBIAS	0.96
drel.	0.96	E_w	0.95
EF	0.33	E_v	0.95
RMSE	0.33	E_p	0.97

2.3.1.1 Topography, Soil and Land Use Data: International Steering Committee for Global Mapping (ISCGM) [31] is the source of DEM used in the present study. IFAS model created river network for Jhelum and Chenab River catchment (i.e., study area) which was remedied utilizing google earth mapping. The land use/cover information, depended upon land cover of Global Twenty land use types of ISCGM, were further classified into five fundamental groups as shown in the Fig. 5. The sub-surface unsaturated tank parameters and aquifer tank parameters are based on soil, surface and depth spread of computerized soil data of the World by FAO-UNESCO, which is also called digital soil map of the world (DSMW) [15,32-33]. The soil classification of the study area according to DSMW, is presented in Fig. 6 (A-B). The soil /geologic data and the land use data were up-scaled to 5×5 km^2 using the framework of IFAS Model.

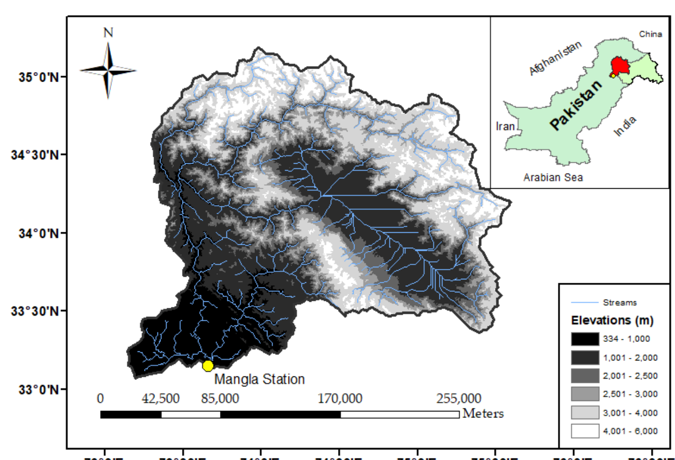

Fig. 3. Location and digital elevation model of Jhelum river basin up to Mangla station

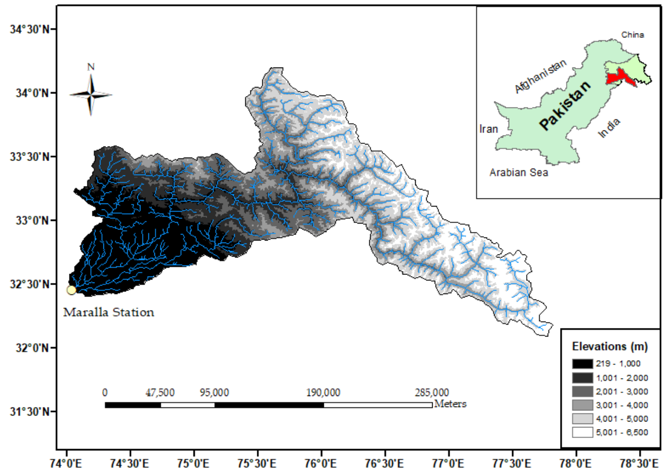

Fig. 4. Location and digital elevation model of Chenab river basin up to Maralla station

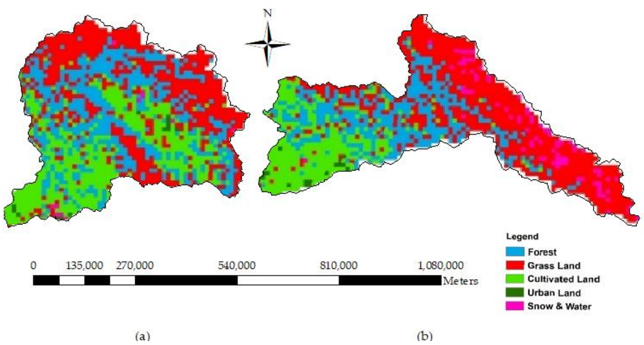

Fig. 5. Land use/cover classification imported in IFAS model (a) Jhelum river basin (b) Chenab river basin

2.3.1.2 Ground observatory rainfall data: Pakistan Meteorological Department (PMD) provided daily precipitation information of twenty two gauging stations inside Pakistan. Eighteen rain gauges provided data of 64.4% (40234 km^2) domain of Jhelum River catchment [34]. To overcome data scarce environment limitations, to some extent, satellite based data (GSMap) has been used with the default parameters to generate the boundary conditions in terms of hydrograph, for the study period, on the grid cell over the river, at the line of control. The successive model simulations for the sensitivity analysis were performed afterwards.

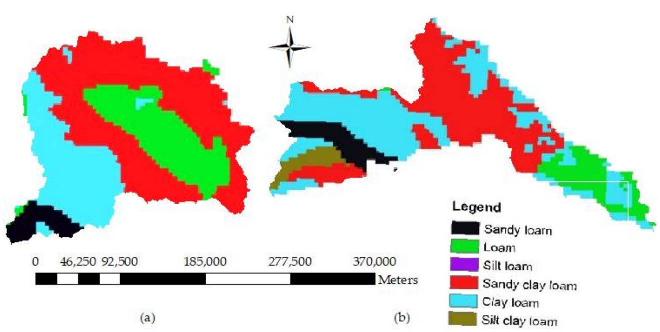

Fig. 6. FAO soil classification (a) Jhelum river basin (b) Chenab river basin

*2.3.1.3 Miscellaneous data (flow, snow cover, temperature, evapotranspiration, grid size and time step)***:** Six hourly measured flow data were collected from Flood Forecasting Division (FFD), Pakistan at two river stations (Mangla, Maralla) in the basins for calibration and validation purposes.

Snowmelt contribution to discharge has been calculated by importing MODIS daily snow cover product and albedo data. The grid size was originally 500m x 500m, which is up-scaled to 5 x 5 km^2, in IFAS model. Aamir et al. [34] presented the sensitivity analysis for the degree-day factors and lapse rate which are used in snow runoff simulations. They presented the results of various other researchers [35-37], who suggested the ranges for degree day factor, critical temperature and lapse rate to calculate snow melt discharge in the region. General value of lapse rate per 100 m and critical temperature is taken as 0.65°C and 4°C respectively.

Maximum and Minimum daily temperature data for 16 gauging stations has been provided by PMD along with the elevations of the stations for snowmelt estimation. Available temperature point data was spatially dispersed utilizing Thiessen polygons method, considering variable altitude of the area as for point elevation data of temperature stations. 30 years information (1979 to 2009) of normal daily evapotranspiration data, provided by National Center for Environmental Prediction's (NCEP) [38], were input in the model.

The simulations were performed in IFAS model on six hourly based precipitation data of the entire monsoon rainfall period. In the year 2014, many areas of Pakistan had encountered one of the severe floods in the history of Pakistan, which brought immense disaster and loss of life and property to the nation. High flood were reported by FFD in Jhelum river and Chenab river. A 5 x 5 km^2 spatial grid is used in the present model.

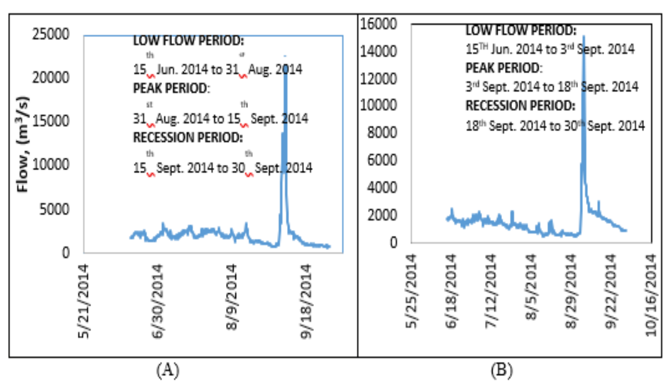

Fig. 7. Classification of flow periods on the observed hydrograph at (a) Maralla station (b) Mangla station (15th June 2014 to 30th September 2014)

3. Result and Discussion

3.1 Assumed Classification of Flow Periods of Stream Discharge Hydrograph

In the present study, the flows at the outlet have been classified as Low flow, Peak flow and Recession flow. Fig. 7 shows the classification of flow periods using the observed data of stream flow at Mangla and Maralla flow measuring stations on Jhelum and Chenab Rivers.

3.2 Results of Parameter Sensitivity Analysis

3.2.1 Application of Kolmogorov-Smirnov test

For Jhelum River and Chenab River basins, the effect of variability of one parameter on the output variability is identified using K-S Test.

The ranking of the parameters based on K-S test for Jhelum River and Chenab river basins are different, but the aquifer layer tank parameters for both the basins have proved to be more sensitive. AGD has the highest value of T_i for Jhelum River and Chenab River basins i.e. 0.62 and 0.4 respectively. HIGD has the second highest ranking in Jhelum River Basin with, T_i value as 0.3. The second highest ranking in Chenab River Basin is for the FALFX parameter of surface layer tank and the T_i value is 0.3. The third and fourth rankings in Jhelum River Basin are for AUD and HCGD respectively, with T_i values of 0.22 and 0.2 respectively. Final infiltration capacity (SKF) is the parameter of surface layer tank. It has proved to be very important parameter in affecting the stream flows in both rivers. T_i value for SKF is 0.2 and 0.175 in Jhelum River and Chenab River respectively.

In the next section, the results of effect of parameter variation in different flow regimes are presented in detail. Further, it also discusses effect of variances of parameter on simulated discharge and the differences of the influence of these parameters in different flow regimes in both basins.

3.2.2 Sensitivity indicators

The results of parameter sensitivity analysis in different flow regimes based on deterministic index and amplification factor are presented in Figs. 8-11.

HIGD, HCGD, are the highly ranked parameters in each flow regime for Jhelum river basin, as shown in the Figs. 8-9, the third highest parameter in every flow regime has turned out to be AGD. It has been observed that in low flow period the parameters role in varying the flow is significant as compared to the peak flow and recession period as shown in the Fig. 8-9. Baseflow increases with increase in HIGD and AGD. During the period of low flow the major portion of the flow is baseflow and the sensitive parameters affecting the baseflows have been determined. The HCGD has the highest value of deterministic index, i.e. it varies from 4.76 to 3.07 in the low flow period, but during the peak and recession periods, its value ranges from 1.15 to 1.17. The second important parameter, on the basis of deterministic index is HIGD. A similar trend of HIGD has also been observed. Its values tend to be high before the peak flow, in low flow period and ranges from 2.34 to 2.88. In the peak and recession periods values are low i.e. 1.46 to 1.0387. The values of AGD are more or less the same in all flow regimes and range from 0.5 to 0.25. Amplification factors, as shown in Fig. 9, presents a similar ranking as that of deterministic index.

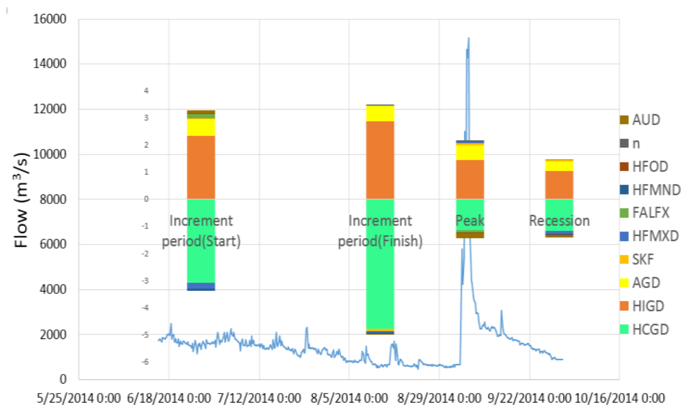

Fig. 8. Sensitivity indices of parameters variation at different flow regimes. Deterministic index for Jhelum river basin

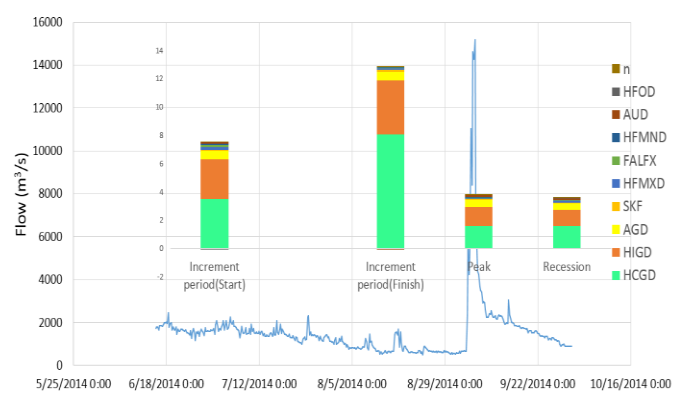

Fig. 9. Sensitivity indices of parameters variation at different flow regimes. Amplification factor for Jhelum river basin

In Chenab River Basin, the highly ranked parameter is HIGD, whose value ranges from 0.72 to 3.708. The least values are in the peak flow, i.e. 0.0702 and 0.95 in the recession period as shown in Fig. 10. The second influential parameter is HCGD whose deterministic index value varies from 0.692 to 3.404 in the low flow period. In the peak flow and recession periods its values are 0.073 and 0.993 respectively. The third important parameter according to deterministic index is AGD. The value of

AGD ranges from 0.408 to 0.506 in the low flow period. In peak flow, it is 0.315 and in the recession period, it is 0.3025. The parameter HFMXD has been observed important in low flow and recession periods, but its values are less than that of AGD. The role of HFMND, during low flow period, has been highlighted by amplification factor, as shown in Fig. 11. The remaining parameters have the same importance ranking as depicted by deterministic index.

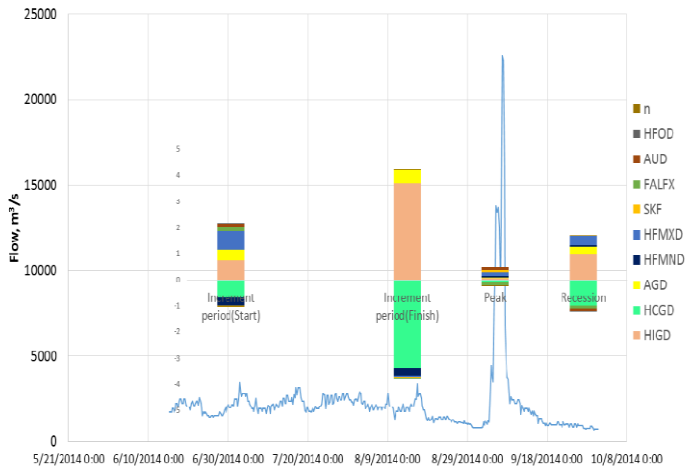

Fig. 10. Sensitivity indices of parameters variation at different flow regimes. Deterministic index for Chenab river basin

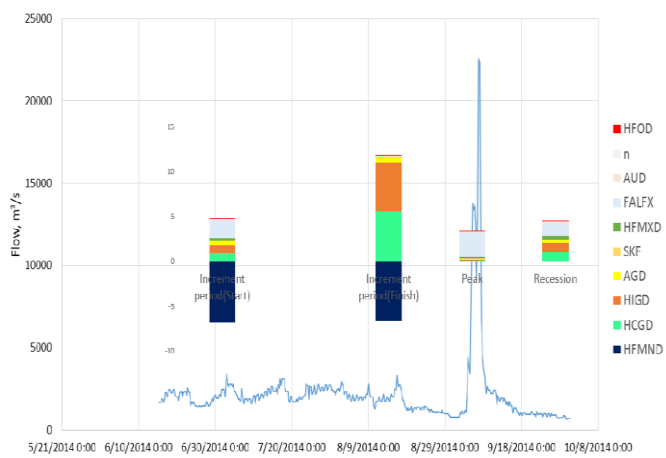

Fig. 11. Sensitivity indices of parameters variation at different flow regimes amplification factor for Chenab river basin

The overall/total effect of parameters is not the same in all the flow regimes in both watersheds. It has been observed that the affect is minimal during the peak flows as compared to low flows. The major portion output flow is calculated or modelled by kinematic wave model during the high flows. The low sensitivity of land use/cover parameters during the peak flow or high flows period has also been endorsed by Ranatunga et al. [39].

3.2.3 Results of Parameter Ranking based on Model Performance Change

The results of parameter ranking based on the rate of change of performance indicators are presented in Fig. 12, where the lighter shades indicates higher ranking. Aquifer tank parameters took the first four ranks for most of the performance plots except peak discharge error. The higher ranking of aquifer parameters (left side) than surface tank parameters (right side) can be observed clearly in Fig. 12. The two redundant parameters for Jhelum River Watershed are HFMND and HFOD.

Criteria	AGD	AUD	HCGD	HIGD	FALFX	HFMND	HFMXD	HFOD	SKF	n
RELATIVE INDEX OF AGREEMENT, drel.	1	7	2	3	8	9	6	10	4	5
MODELING EFFICIENCY, EF.	1	4	2	3	6	10	5	9	7	8
ROOT MEAN SQUARE ERROR, RMSE, m^3/s.	1	4	2	3	6	10	5	9	7	8
RMSE/STDEVobs , RSR.	1	4	2	3	6	10	5	9	7	8
FOURTH ROOT MEAN QUADRUPPLED ERROR,	2	1	4	6	5	10	3	9	7	8
PERCENT BIAS, PBIAS, %.	3	8	2	1	5	10	4	7	6	9
WAVE SHAPE ERROR, ew.	1	4	2	3	7	10	6	9	5	8
VOLUME ERROR, ev.	3	8	2	1	5	10	4	7	6	9
PEAK DISCHARGE ERROR, ep.	6	1	5	7	2	10	8	9	3	4

Legend	1	2	3	4	5	6	7	8	9	10

(a)

Criteria	AGD	AUD	HCGD	HIGD	FALFX	HFMND	HFMXD	HFOD	SKF	n
RELATIVE INDEX OF AGREEMENT, drel.	3	9	1	2	7	8	5	10	4	6
MODELING EFFICIENCY, EF.	3	4	2	1	8	10	6	9	5	7
.ROOT MEAN SQUARE ERROR,	3	4	2	1	7	10	5	9	6	8
RMSE/STDEVobs , RSR.	3	4	2	1	7	10	5	9	6	8
FOURTH ROOT MEAN	7	1	4	6	3	10	2	8	5	9
PERCENT BIAS, PBIAS, %.	3	10	1	2	4	8	5	7	6	9
WAVE SHAPE ERROR, e_w.	2	5	1	3	9	7	6	10	4	8
VOLUME ERROR, e_v.	3	10	1	2	4	8	5	7	6	9
PEAK DISCHARGE ERROR, e_p.	9	1	5	6	7	10	2	8	3	4

Legend	1	2	3	4	5	6	7	8	9	10

(b)

Fig. 12. Parameter ranking based on slope of performance plots (a) Jhelum river basin (b) Chenab river basin

Chenab River Basin also presents a similar trend of parameter ranking (Fig. 12 (b)). Aquifer tank parameters HCGD, HIGD, AGD are highly ranked parameters and the two most redundant parameters in Chenab River Basin are again identified as HFMND and HFOD.

3.2.4 Optimal parameterization and interpolating linear regression metamodels

In present study, metamodels, are the linear regression equations which were obtained using the results and the objective functions of sensitivity experiments (deterministic index and amplification factor). These linear regression equations, served as Metamodels, provided the relationship between the parameters and the stream flows. The values of most sensitive parameters, were evaluated for high observed flows and low observed flows, using these Metamodels, in each of the basins.

The coefficient of determination, R^2, was the goodness of fit index of the linear regression metamodels, for highly ranked parameters. The values of R^2 of all the metamodels, for both basins, are more than 0.86 for high flows and more than 0.71 for low flows. It is also observed that in all Metamodels types, the linear relationship is preserved even when the parameters are varying at a very high level. The optimum ranges of these parameters for each basin, are shown in Table 5.

Table 5

Optimized ranges for highly ranked parameters in Jhelum river basin and Chenab river basin

Jhelum River Watershed	Optimal Ranges	Chenab River Watershed	Optimal Ranges
AGD, Coefficient for base flow	0.0016-0.0092	HFMXD, Maximum water height	0.005-0.011
AUD, Slow subsurface flow Regulation coefficient	0.1145-0.1629	HIGD, Initial water height on aquifer layer tank	1.63-1.98
HCGD, Height where slow subsurface flow occurs	1.6-1.63	HCGD, Height where slow subsurface flow occurs	1.83-2.52
HIGD, Initial water height on aquifer layer tank	2.38-2.4	AUD, Slow subsurface flow Regulation coefficient	0.5-0.8

3.2.5 Calibration and validation results

The calibration has been performed for the period from 15th June 2014 to 30th October 2014 and the validation period is 15th June 2013 to 30th October 2013. All the three types of metamodels gave the same ranges for the HCGD parameter. However, for the others parameters such as AGD, AUD and HIGD, all metamodels provided different ranges of values. Further, all metamodels optimized and compressed the ranges of parameter space. Calibration results of both basins are in very good range of Nash Suttcliff Coefficient, NSE and coefficient of determination, R^2. At Mangla Dam Station in Jhelum River, model is calibrated for output stream flows, for the year 2014, with the NSE and R^2 values as 0.829 and 0.813 respectively. The validation of model is performed for the year 2013, with NSE and R^2 values as 0.78 and 0.72 respectively. The IFAS is calibrated using the observed flows at Maralla Barrage station in Chenab River, for the year 2014, with NSE and R^2 values as 0.79 and 0.81 respectively. The validation results of NSE and R^2 values, on Chenab river, for the year 2013, are 0.82 and 0.83 respectively.

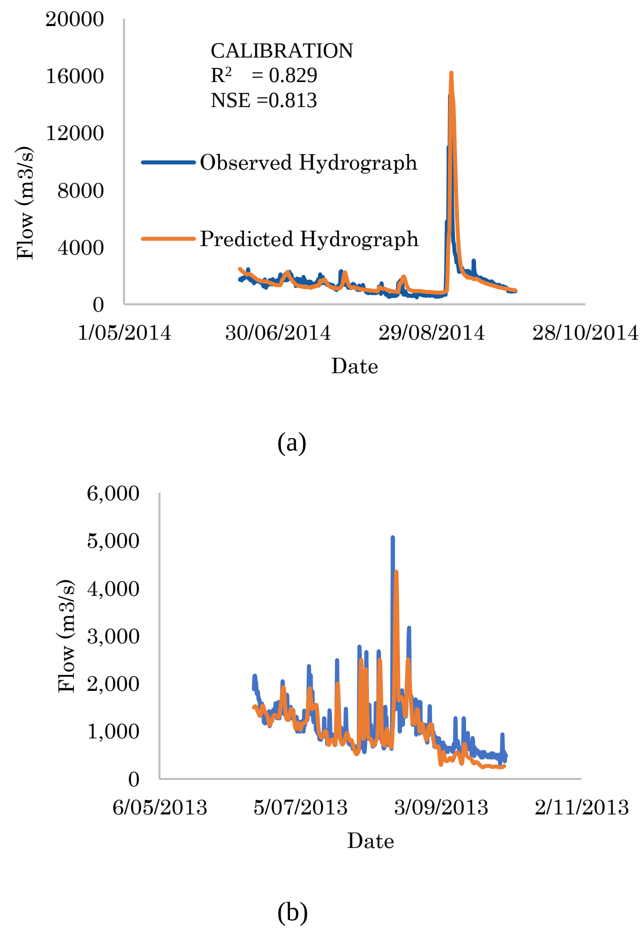

Fig. 13. (a) Calibration (for year 2014) and (b) validation (for year 2013) results in Mangla dam station

4. Conclusion

The present study introduces a robust method which integrates the sensitivity analysis with the optimization algorithm. It not only deliver a set of highly sensitive hydrogeological parameters for high and low flow regimes, but also the ranges of these highly sensitive parameters using the objective functions, or metamodels, that further help in reducing the optimization runs of the highly resolved distributed hydrological models.

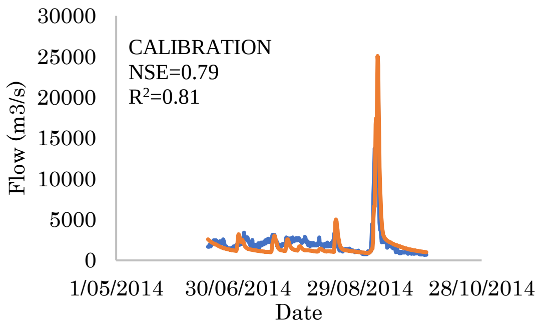

(a)

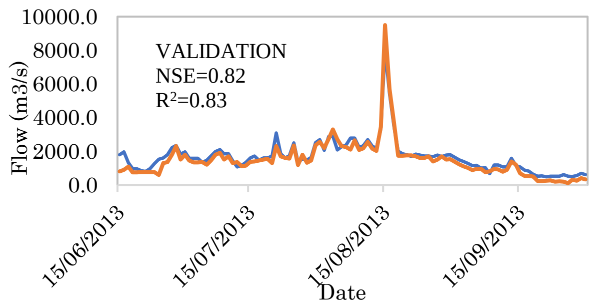

(b)

Fig. 14. (a) Calibration (for the monsoon period of year 2014) and (b) Validation results (for the monsoon period of year 2013) in Maralla station

The investigation gives an improved comprehension of the IFAS model and a knowledge into which model parameters are critical. In this manner, this investigation gives a more profound understanding into the modelling system. Different sensitivity experiments poses the ranking of the parameters which helps the modelers to incorporate the change in highly influenced parameters. The results proved that the analysis should be directed independently for each study basin as the sensitivity results are not transferable among catchments and flow periods.

The sensitivity analysis of the hydrogeological parameters of IFAS model, for the assessment of effectiveness of the parameters to produce the model output, is of great importance in optimizing and estimating the model parameters. The sensitivity of these parameters are varying spatially as well as temporally. The sensitivity indices for all parameters are observed to be different in different flow periods and for different watersheds.

Sensitivity analyses identified the parameters of aquifer layer tank (HCGD, HIGD, AGD, AUD) which are playing very important roles in the streamflow equations. Regression analysis results indicated that these parameters are negatively or positively correlated with the output flow. Parameter optimization has been performed through the use of different metamodels obtained from the sensitivity experiments, which gave the effective range of parameter values, that can be used for calibration and parameterization processes. It is also observed that in all of the types of Metamodels, the linear relationship between the output change statistics with input parameter change statistics, is persistent even in the high change of parameter value. In this case, linear regression Metamodels have provided reliable algorithm for the model parameters optimization. The calibration and validation results show that the methodology employed to determine the optimized parameter is quiet supportive for accurate calibration.

The analysis revealed that the aquifer parameters and the parameters related to rapid sub-surface flow and infiltration are playing crucial and significant role during low flow periods than in high flow periods for both watershed i.e. Jhelum River and Chenab River Basins. For efficient and reliable optimization algorithms, sensitivity analysis plays vital role in estimating the effects of parameters on model predictions. IFAS model is an efficient model to simulate subsurface as well overland flow. A subject for future studies can be characterization and propagation of uncertainty due to temporal and spatial data input.

5. References

[1] X. Song, J. Zhang, C. Zhan, Y. Xuan, M. Ye, and C. Xu, “Global sensitivity analysis in hydrological modeling: Review of concepts, methods, theoretical framework, and applications”, Journal of Hydrology, vol. 523, pp. 739–757, 2015.

[2] S. Razavi, B. A. Tolson, and D. H. Burn, “Review of surrogate modeling in water resources”, Water Resources Research, vol. 48, no. 7. 2012.

[3] L. T. Ha, W. G. M. Bastiaanssen, A. van Griensven, A. I. J. M. van Dijk, and G. B. Senay, “Calibration of spatially distributed hydrological processes and model parameters in SWAT using remote sensing data and an auto-calibration procedure: a case study in a vietnamese river basin”, Water, vol. 10, no. 2, 2018.

[4] S. Wang, G. (Gordon) Huang, B. W. Baetz, and B. C. Ancell, “Towards robust quantification and reduction of uncertainty in hydrologic predictions: Integration of particle Markov chain Monte Carlo and factorial polynomial chaos expansion”, Journal of Hydrology, vol. 548, pp. 484–497, 2017.

[5] J.-P. Gauchi, A. Bensadoun, F. Colas, and N. Colbach, “Metamodeling and global sensitivity analysis for computer models with correlated inputs: A practical approach tested with a 3D light interception computer model”, Environmental Modelling and Software, vol. 92, pp. 40–56, 2017.

[6] D. P. Boyle, H. v. Gupta, and S. Sorooshian, “Toward improved calibration of hydrologic models: Combining the strengths of manual and automatic methods”, Water Resources Research, vol. 36, no. 12, pp. 3663–3674, 2000.

[7] T. S. Hogue, S. Sorooshian, H. Gupta, and A. Holz, “A multistep automatic calibration scheme for river forecasting models”, Journal of Hydrometeorology, vol. 1, pp. 524-542, 2020

[8] P. O. Yapo, H. V. Gupta, and S. Sorooshian, “Multi-objective global optimization for hydrologic models”, Journal of Hydrology, vol. 204, no. 1, pp. 83–97, 1998.

[9] F. Fenicia, H. H. G. Savenije, P. Matgen, and L. Pfister, “A comparison of alternative multiobjective calibration strategies for hydrological modeling”, Water Resources Research, vol. 43, no. 3, DOI: 10.1029/2006WR005098, 2007.

[10] M. Ahmed and S. A. A. Zaidi, “Calibration and validation of an experimental setup for the measurement of the cylindrical body shapes and curvatures of the objects and subjects through the techniques of rasterstereography”, Mehran University Research Journal of Engineering and Technology, vol. 38, no. 1, pp. 197–208, 2019.

[11] M. Ali Rajper, A. Ghafoor Memon, K. Harijan, and J. Power Company Limited, “Exergy analysis of a subcritical reheat steam power plant with regression modeling and optimization”. Mehran University Research Journal of Engineering and Technology, vol. 35, no. 3, pp. 459–472, 2016.

[12] Q. Javaid, A. Zafar, M. Awais, and M. A. Shah, “Cache memory: an analysis on replacement algorithms and optimization techniques”, Mehran University Research Journal of Engineering and Technology, vol. 36, no. 4, pp. 831–840, 2017.

[13] M. Mughees, F. Gohar Awan, and A. Mughees, “Volt/VAr optimization of distribution system with integrated distributed generation”, Mehran University Research Journal of Engineering and Technology, vol. 36, no. 1, pp. 117–128, 2017.

[14] H. Jalal, B. Dowd, F. Sainfort, and K. M. Kuntz, “Linear regression metamodeling as a tool to Summarize and present simulation model results”, Medical Decision Making, vol. 33, no. 7, pp. 880–890, 2013.

[15] K. Fukami, T. Sugiura, J. Magome, and T. Kawakami, “Integrated flood analysis system”, IFAS version 1.2 user’s manual.

[16] M. Sugawara, “Automatic calibration of the tank model”, Hydrological Sciences Bulletin, vol. 24, no. 3, pp. 375–388, 1979.

[17] T. Fukuda, R. Jayadi, Y. Nakano, and M. Kuroda, “Application of complex tank model for evaluating performance of water operation in a reused water irrigation system”, Journal of the Faculty of Agriculture, Kyushu University, vol. 44, no. 1–2, pp. 189–198, 1999.

[18] P. Chiu, “Investigation best number of tanks for hydrological tank model for rural catchment in humid region”, 2011.

[19] H. Basri, “Development of rainfall-runoff modeling using a tank model: problems and challenges in province of aceh, Indonesia”, Aceh International Journal of Science and Technology, vol. 2, no. 1, pp. 26–37, 2013.

[20] A. Sugiura, S. Fujioka, S. Nabesaka, M. Tsuda, and Y. Iwami, “Development of a flood forecasting system on the upper Indus catchment using IFAS”, Journal of Flood Risk Management, vol. 9, no. 3, pp. 265–277, 2016.

[21] S. Devaliya, H. L. Tiwari, and A. Balvanshi, “Runoff estimation of a basin using tank model”, International Journal of Emerging Research in Management and Technology, vol. 6, no. 5, pp. 51–53, 2017.

[22] H. T. Phuong, N. X. Tien, H. Chikamori, and K. Okubo, “A hydrological tank model assessing historical runoff variation in the hieu river basin”, Asian Journal of Water, Environment and Pollution, vol. 15, no. 1, pp. 75–86, 2018.

[23] F. Pianosi et al., “Sensitivity analysis of environmental models: A systematic review with practical workflow”, Environmental Modelling & Software, vol. 79, pp. 214–232, 2016.

[24] K. K. Benke, K. E. Lowell, and A. J. Hamilton, "Parameter uncertainty, sensitivity analysis and prediction error in a water-balance hydrological model", Mathematical and Computer Modelling, vol. 47, no. 11–12, pp. 1134–1149, 2008.

[25] W. Panichkitkosolkul, "Confidence intervals for the coefficient of variation in a normal distribution with a known population mean", Journal of Probability and Statistics, vol. 2013, pp. 1–11, 2013.

[26] F. Pianosi and T. Wagener, "A simple and efficient method for global sensitivity analysis based on cumulative distribution functions", Environmental Modelling & Software, vol. 67, pp. 1–11, 2015.

[27] D. Jung, Y. Choi, and J. Kim, "Multiobjective automatic parameter calibration of a hydrological model", Water, vol. 9, no. 3, p. 187, 2017.

[28] E. Roszkowska, "Rank ordering criteria weighting methods – a comparative overview", Optimum. Studia Ekonomiczne, no. 5(65), pp. 14–33, 2013.

[29] A. Wang and D. P. Solomatine, "Practical experience of sensitivity analysis: comparing six methods, on three hydrological models, with three performance criteria". Water, vol. 11, no. 5, p. 1062, 2019.

[30] M. Nawaz, R. J. Wasson, R. Bhushan, N. Juyal, and F. Sattar, "Topsoil delivery to Himalayan rivers: the importance of sampling time", Hydrological Processes, vol. 30, no. 24, pp. 4609–4616, 2016.

[31] "Elevation - global version - global map". https://globalmaps.github.io/el.html [Accessed Mar.11, 2022].

[32] "FAO/UNESCO soil map of the world | FAO soils portal | food and agriculture organization of the United Nations". https://www.fao.org/soils-portal/soil-survey/soil-maps-and-databases/faounesco-soil-map-of-the-world/en/ [Accessed Mar 11, 2022].

[33] T. Sugiura, K. Fukami, and H. Inomata, "Development of integrated flood analysis system (IFAS) and its applications", World Environmental and Water Resources Congress 2008: Ahupua'a - Proceedings of the World Environmental and Water Resources Congress 2008, vol. 316, pp. 1–10, 2008.

[34] A. Shahzad, H. F. Gabriel, S. Haider, A. Mubeen, and M. J. Siddiqui, "Development of a flood forecasting system using IFAS: a case study of scarcely gauged Jhelum and Chenab river basins", Arabian Journal of Geosciences, vol. 11, no. 14, pp. 1–18, 2018.

[35] M. Azmat, M. U. Qamar, C. Huggel, and E. Hussain, "Future climate and cryosphere impacts on the hydrology of a scarcely gauged catchment on the Jhelum river basin, Northern Pakistan", Science of The Total Environment, vol. 639, pp. 961–976, 2018.

[36] T. Liu, M. Tsuda, and Y. Iwami, "A study on flood forecasting in the upper indus basin considering snow and glacier meltwater", Journal of Disaster Research, vol. 12, no. 4, pp. 793–805, 2017.

[37] D. R. Archer and H. J. Fowler, "Using meteorological data to forecast seasonal runoff on the River Jhelum, Pakistan", Journal of Hydrology, vol. 361, no. 1–2, pp. 10–23, 2008.

[38] M. Kanamitsu *et al.*, "NCEP–DOE AMIP-II reanalysis (R-2)", Bulletin of the American Meteorological Society, vol. 83, no. 11, pp. 1631–1644, 2002.

[39] T. Ranatunga, S. T. Y. Tong, and Y. J. Yang, "An approach to measure parameter sensitivity in watershed hydrological modelling", vol. 62, no. 1, pp. 76–92, 2016.

